

HEAVY-ION REACTIONS AS A TECHNIQUE FOR DIRECT MASS MEASUREMENTS
OF UNKNOWN $Z > N$ NUCLEI

Joseph Cerny,* C. U. Cardinal, K. P. Jackson, D. K. Scott, and A. C. Shotter
Nuclear Physics Laboratory, University of Oxford, Oxford, England
(Received 13 July 1970)

The reactions $^{40}\text{Ca}(^{12}\text{C}, t)^{49}\text{Mn}$ and $^{40}\text{Ca}(^{12}\text{C}, ^3\text{He})^{49}\text{Cr}$ have been observed with ground-state cross sections of the order of $1 \mu\text{b}/\text{sr}$. The results for ^{49}Mn are consistent with its predicted mass excess of $-37.72 \pm 0.08 \text{ MeV}$.

Almost nothing is known concerning the properties of $Z > N$ nuclei above the titanium isotopes. In fact, no technique has yet been demonstrated in this region which permits even the mass measurement of the $T_z = \frac{1}{2}(N-Z) = -\frac{1}{2}$ members of the $T_z = \pm \frac{1}{2}$ mirror pairs. These masses are of importance to various theoretical mass equations (e.g., Kelson and Garvey¹) and the systematics of Coulomb displacement energies. We would like to report the feasibility of heavy-ion-induced reactions for this purpose. As an initial experiment, we have chosen the reaction $^{40}\text{Ca}(^{12}\text{C}, t)^{49}\text{Mn}$ as a means of studying the hitherto uncharacterized² nuclide ^{49}Mn ; our results agree well with the theoretical prediction of its mass.

Preliminary experiments had indicated a fairly low cross section for the $(^{12}\text{C}, t)$ reaction on ^{40}Ca . Due to this, simultaneous measurements of both the reactions $^{40}\text{Ca}(^{12}\text{C}, t)^{49}\text{Mn}$ and $^{40}\text{Ca}(^{12}\text{C}, ^3\text{He})^{49}\text{Cr}$ leading to mirror final states were made. Both reactions presumably proceed by the same mechanism, and observation of the latter reaction—which produces known final states, but which is experimentally more difficult—was taken as a measure of the experimental reliability. Further, it was necessary to employ particle identification techniques appropriate to low cross-section measurements.³

A $^{12}\text{C}^{4+}$ beam with an intensity of $\approx 150 \text{ nA}$ at an energy of 27.5 MeV ⁴ from the Oxford EN tandem Van de Graaff was used to irradiate $150\text{-}\mu\text{g}/\text{cm}^2$ targets of Ca evaporated on $500\text{-}\mu\text{g}/\text{cm}^2$ Au backings. Reaction products were observed in a counter telescope consisting of four semiconductor detectors: two ΔE detectors denoted $\Delta E1$ and $\Delta E2$ of 60 and 50 μm thickness, respectively; an E detector 935 μm thick; and a rejection detector for long-range reaction products traversing the first three detectors. An Al foil 9.4 mg/cm^2 thick was placed in front of this telescope to remove elastically scattered ^{12}C ions.

Two separate identifications of each particle stopping in the system were made with the method of Fisher and Scott.⁵ One identification (denoted

M1) employed the summed pulses from the first two detectors as its ΔE signal, while the other (denoted M2) utilized the pulse from the $\Delta E2$ detector alone as its ΔE signal. These two identification signals and the total energy signal for each event were sent via separate ADC's to a PDP-7 computer operating to a multiparameter mode. Partial analysis of these data was possible on line with the associated IBM disc, and all events were stored on magnetic tape for extensive off-line analysis with a PDP-10 computer. Analysis of the relevant energy spectra, after taking into account data from both identifications, is necessary when investigating very low-yield reaction products arising from relatively endothermic reactions; otherwise some events, due basically to much higher yield reaction products but resulting in unusual energy loss in a single ΔE detector, can simulate the particles of interest and obscure their energy spectra.³

Figure 1 shows M2 particle identification spectra arising from ^{12}C reactions on a Ca target and its ^{12}C and ^{16}O contaminants. Limits for selection of the different particle groups were determined by using the reaction of 15-MeV ^3He on $^{10,11}\text{B}$ which produces a more uniform yield of the different particles (for this run the Al foil was removed). As expected, proton and ^4He emission dominated the composite identifier spectra from reactions induced by the ^{12}C beam. The protons are not shown in Fig. 1 [curve (b)] since their relative yield in these final data is not representative due to various thresholds required for acceptable energy loss in the ΔE and E detectors. The overall selection necessary to obtain relatively clean triton and ^3He energy spectra resulted in a maximum possible "loss" of 40 and 50%, respectively, of probable true events.

Figures 2(a) and 2(b) present triton and ^3He energy spectra arising at 16° (lab) from ^{12}C reactions on ^{40}Ca . The most energetic peaks, albeit with poor statistics, shift appropriately with angle between 7° and 40° (lab); kinematically compensated composite spectra for both reac-

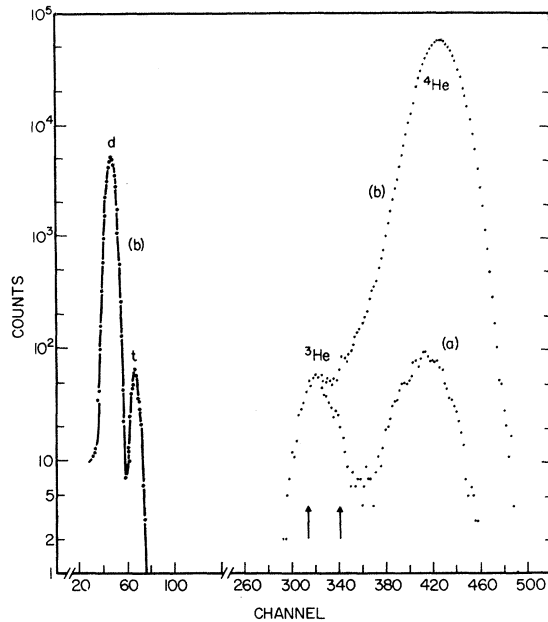


FIG. 1. Particle identification spectra from the 27.5-MeV ^{12}C reaction on a Ca target and its ^{12}C and ^{16}O contaminants. A counter telescope incorporating two ΔE detectors has been employed as discussed in the text. Curve (a) presents those events remaining in the M2 identification spectrum *after* a gate has been set around the ^3He region in the M1 identification; the final ^3He energy spectra then arise from a selection from the data in this M2 spectrum with limits set as indicated by the arrows. Curve (b) presents a composite M2 identification spectrum obtained by adding spectra for all the particle types after appropriate limits have been set on the M1 data.

tions are shown in Figs. 2(c) and 2(d).

Deuteron and ^4He data from ^{12}C -induced reactions, as well as energy spectra of all particles of interest from the $^{10,11}\text{B} + ^3\text{He}$ reaction, established an energy calibration. This calibration was used to provide absolute energy determinations for both the $(^{12}\text{C}, t)$ and $(^{12}\text{C}, ^3\text{He})$ reactions. The predicted locations of the known⁶ ground and low-lying states of ^{49}Cr are indicated in Figs. 2(b) and 2(d). Although there is a high background in the ^3He data (discussed further below), these absolute predictions agree acceptably with the locations of the major higher-energy structure at all observed angles. Completely independently, the predicted position of the $^{40}\text{Ca}(^{12}\text{C}, t)^{49}\text{Mn}(\text{g.s.})$ transition is indicated in Figs. 2(a) and 2(c); this prediction is based on a ^{49}Mn mass excess of -37.72 ± 0.08 MeV obtained from Coulomb displacement energy systematics and theoretical calculations.⁷ Again, agreement with the major higher-energy structure can be

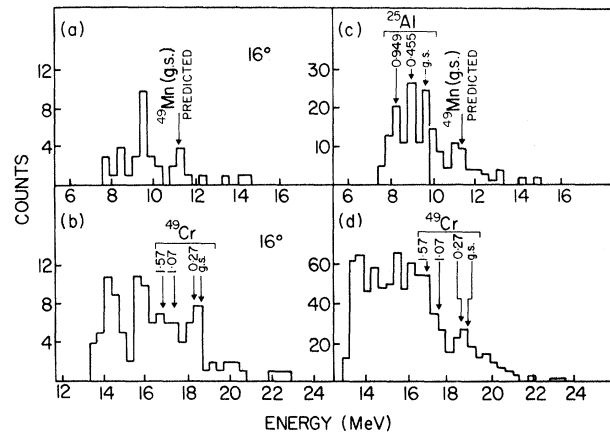


FIG. 2. (a) $^{40}\text{Ca}(^{12}\text{C}, t)^{49}\text{Mn}$ and (b) $^{40}\text{Ca}(^{12}\text{C}, ^3\text{He})^{49}\text{Cr}$ energy spectra at 16° . As discussed in the text, the predicted locations of *known* final states in ^{49}Cr as well as the predicted location of the $^{49}\text{Mn}(\text{g.s.})$ are indicated. The peak near 9.5 MeV in (a) arises at least in part from the reaction $^{16}\text{O}(^{12}\text{C}, t)^{25}\text{Al}$. (c) Composite energy spectra for the reactions $^{40}\text{Ca}(^{12}\text{C}, t)^{49}\text{Mn}$ and (d) $^{40}\text{Ca}(^{12}\text{C}, ^3\text{He})^{49}\text{Cr}$, as well as for the contaminant reaction $^{16}\text{O}(^{12}\text{C}, t)^{25}\text{Al}$, obtained from kinematically correcting to 7° data taken at angles from 7° to 40° . The lower part of the triton spectrum is kinematically corrected appropriate to reactions on ^{16}O while the upper part is corrected for reactions on ^{40}Ca . Transitions to the various final states are indicated as in (a) and (b).

observed. Some of the background events above the ground states in Fig. 2 may arise from reactions on the other Ca isotopes present in this natural Ca target and some ^4He continuum "leak through" may still be present in the ^3He data. The much higher yield reactions on the light target contaminants ^{12}C and ^{16}O —which almost obscure transitions to low-lying states in the reaction $^{40}\text{Ca}(^{12}\text{C}, ^4\text{He})^{48}\text{Cr}$ —do not interfere with these spectra due to Q -value and kinematic effects. In fact, only the reaction $^{16}\text{O}(^{12}\text{C}, t)^{25}\text{Al}$ appears in these data significantly above the low-energy cutoff.

The general experimental conditions necessitated by the low yield resulted in the poor energy resolution of ≈ 300 keV as measured for ^4He groups. As such, the $^{40}\text{Ca}(^{12}\text{C}, ^3\text{He})^{49}\text{Cr}(\text{g.s.}, \frac{5}{2}^-)$ and $^{49}\text{Cr}^*(0.27 \text{ MeV}, \frac{7}{2}^-)$ transitions could not be resolved, though the results are consistent with a roughly comparable population of both states (in agreement with the anticipated strong influence of a $2J_f + 1$ statistical weighting). The $(^{12}\text{C}, t)$ data on the mirror nucleus ^{49}Mn are also consistent with population of the predicted⁷ ground state and an assumed first excited state at an equivalent excitation to that for its mirror in

^{49}Cr . (Centroid analysis of these two states – assumed to be equally populated – yields a mass excess for ^{49}Mn differing from that in Ref. 7 by ≈ 50 keV.) Average differential cross sections to the summed ground and first excited states are $\approx 1.5 \mu\text{b/sr}$ (for tritons) and $\approx 3 \mu\text{b/sr}$ (for ^3He).

These results demonstrate the practicability of direct mass measurements of $Z > N$ nuclei above Ti using heavy-ion-induced reactions. By extension of these investigations to the use of ^{14}N and ^{16}O projectiles as well as to more exotic reactions such as $^{40}\text{Ca}(^{12}\text{C}, ^6\text{He})^{46}\text{Cr}$, $^{40}\text{Ca}(^{12}\text{C}, ^8\text{He})^{44}\text{Cr}$, etc., it should be possible to determine nuclear masses and their agreement with theoretical prediction in regions of high Coulomb energy very far from the valley of stability.

We are grateful to Professor D. H. Wilkinson and Professor K. W. Allen for the use of the Oxford EN tandem. C. U. Cardinal wishes to thank the National Research Council of Canada for a Postdoctoral Fellowship; D. K. Scott wishes to thank Balliol College, Oxford, for a Junior Research Fellowship; and A. C. Shotton wishes to thank the Science Research Council for a Post-

doctoral Fellowship.

*1969–1970 John Simon Guggenheim Fellow. Permanent address: Department of Chemistry and Lawrence Radiation Laboratory, University of California, Berkeley, Calif.

¹I. Kelson and G. T. Garvey, *Phys. Lett.* **23**, 689 (1966).

²There is one previous reference to ^{49}Mn known to us [H. Tyrén and P. A. Tove, *Phys. Rev.* **96**, 773 (1954)]. These preliminary data on its half-life may in fact arise from or be dominated by the decay of ^{46}V . See C. M. Lederer, J. M. Hollander, and I. Perlman, *Table of Isotopes* (Wiley, New York, 1967), 6th ed.

³G. W. Butler, J. Cerny, S. W. Cosper, and R. L. McGrath, *Phys. Rev.* **166**, 1096 (1968).

⁴Machine limitations made this the maximum available energy. The Coulomb barrier for the reaction on ^{40}Ca based on a radius parameter r_0 of 1.5 fm is 26.2 MeV (lab). See also T. D. Thomas, *Phys. Rev.* **116**, 703 (1959).

⁵P. S. Fisher and D. K. Scott, *Nucl. Instrum. Methods* **49**, 301 (1967).

⁶P. David, H. H. Duhm, R. Bock, and R. Stock, *Nucl. Phys.* **128A**, 47 (1969)

⁷M. Harchol, A. A. Jaffe, J. Miron, I. Unna, and J. Zioni, *Nucl. Phys.* **90A**, 459 (1967).

STRUCTURE OF THE POTENTIAL ENERGY SURFACE AT LARGE DEFORMATIONS*

Ulrich Mosel

Department of Physics and Astronomy, The University of Tennessee, Knoxville, Tennessee 37902, and Oak Ridge National Laboratory, Oak Ridge, Tennessee 37830

and

Dieter Scharnweber

Institute für Theoretische Physik der Universität Frankfurt, Frankfurt am Main, Germany

(Received 6 July 1970)

The two-center shell model has been generalized to the shape of two overlapping spheroids with equal mass. In this model shell corrections have been calculated and the potential energy surface of two heavy nuclei has been investigated. The influence of fragment shells in the model gives rise to structure in this surface which supports assumptions of earlier models for the scission point.

In recent years much new effort has been put into the calculation of shell effects in the nuclear potential-energy surface.^{1,2} These calculations begin with well-known shell models and extend them to the inclusion of deformed shapes of the fissioning nucleus by simply deforming the equipotential surfaces in a uniform way. Only very recently a new model has been proposed^{3,4} which, in contrast to these, can describe the entire course of a fissioning nucleus from its ground state to stages beyond scission.

In this paper the schematic shapes of Ref. 3 have been generalized to the configuration of two

overlapping spheroids with equal mass. This same family of shapes has been investigated very extensively and carefully by Nix and Swiatecki⁵ in the liquid-drop model (LDM).

The Hamiltonian operator of the model is

$$H = T + \frac{1}{2}m\omega_\rho^2\rho^2 + \frac{1}{2}m\omega_z^2(|z|-z_0)^2 + V(\vec{l}, \vec{s}), \quad (1)$$

with

$$V(\vec{l}, \vec{s}) = \begin{cases} C\vec{l}_1 \cdot \vec{s} + D[\vec{l}_1^2 - \frac{1}{2}N(N+3)], & z > 0, \\ C\vec{l}_2 \cdot \vec{s} + D[\vec{l}_2^2 - \frac{1}{2}N(N+3)], & z < 0. \end{cases} \quad (2)$$

Here \vec{l}_1 and \vec{l}_2 describe the angular momenta with